DMD Fast Forward. Published on October 2, 2019 as DOI: 10.1124/dmd.119.088351
This article has not been copyedited and formatted. The final version may differ from this version.

The role of L- and D-menthol in the glucuronidation and detoxification of the major lung carcinogen, NNAL

Shannon Kozlovich, Gang Chen, Christy JW Watson, William J Blot and Philip Lazarus

Department of Pharmaceutical Sciences, College of Pharmacy and Pharmaceutical Sciences, Washington State University, Spokane WA (SK, GC, CW, PL)

Division of Epidemiology, Vanderbilt University Medical Center, Nashville TN (WB)

DMD Fast Forward. Published on October 2, 2019 as DOI: 10.1124/dmd.119.088351
This article has not been copyedited and formatted. The final version may differ from this version.

Running Title: L- and D-menthol inhibit detoxification of tobacco carcinogens

Corresponding author: Philip Lazarus, Ph.D., Department of Pharmaceutical Sciences, College of Pharmacy and Pharmaceutical Sciences, Washington State University; 412 E. Spokane Falls Blvd, Spokane WA 99210; Phone: (509) 358-7947; Email: phil.lazarus@wsu.edu

Manuscript Details:

Text pages - 20

Tables – 5

Figures – 4

Supplemental Figures and Tables – 3

References – 66

Abstract – 250 words

Introduction – 1110 words

Discussion – 1308 words

Abbreviations: 4-(methylnitrosamino)-1-(3-pyridyl)-1-butanol (NNK), 4-(methylnitrosamino)-1-(3-pyridyl)-1-butanone (NNAL), human intestinal microsomes (HIM), human liver microsomes (HLM), Internal Standard (IS), menthol glucuronides (MG), tobacco specific nitrosamines (TSNA), UDP-glucuronosyltransferase (UGT), liquid chromatography mass spectrometry (LC-MS/MS)

DMD Fast Forward. Published on October 2, 2019 as DOI: 10.1124/dmd.119.088351
This article has not been copyedited and formatted. The final version may differ from this version.

ABSTRACT

Menthol, which creates mint flavor and scent, is often added to tobacco in both menthol and non-menthol cigarettes. 4-(methylnitrosamino)-1-(3-pyridyl)-1-butanone (NNK), a potent tobacco carcinogen, is extensively metabolized to its equally carcinogenic metabolite 4-(methylnitrosamino)-1-(3-pyridyl)-1-butanol (NNAL) as (*R*)- or (*S*)-NNAL enantiomers. NNAL is detoxified by UDP-glucuronosyltransferase (UGT) enzymes with glucuronidation occurring on either NNAL's pyridine ring nitrogen (NNAL-*N*-Gluc) or the chiral alcohol [(*R*)- or (*S*)-NNAL-*O*-Gluc]. To characterize a potential effect by menthol on NNAL glucuronidation, *in vitro* menthol glucuronidation assays and menthol inhibition of NNAL-Gluc formation assays were performed. Additionally, NNAL and menthol glucuronides (MG) were measured in the urine of smokers (n=100) from the Southern Community Cohort Study. UGTs 1A9, 1A10, 2A1, 2A2, 2A3, 2B4, 2B7 and 2B17 all exhibited glucuronidating activity against both L- and D-menthol. In human liver microsomes, both L- and D-menthol inhibited the formation of each NNAL-Gluc, with a stereospecific difference observed between the formation of (*R*)-NNAL-*O*-Gluc and (*S*)-NNAL-*O*-Gluc in the presence of D-menthol but not L-menthol. With the exception of three non-menthol cigarette smokers, urinary MG was detected in all menthol and non-menthol smokers, with L-MG comprising >98% of total urinary MG. Levels of urinary NNAL-*N*-Gluc were significantly ($p<0.05$) lower among subjects with high levels of total urinary MG; no significant changes in free NNAL were observed. These data suggest that the presence of menthol could lead to increases in alternative, activating metabolic pathways of NNAL in tobacco target tissues, increasing the opportunity for NNAL to damage DNA and lead to the development of tobacco-related cancers.

DMD Fast Forward. Published on October 2, 2019 as DOI: 10.1124/dmd.119.088351
This article has not been copyedited and formatted. The final version may differ from this version.

SIGNIFIGANCE

High levels of the major menthol metabolite, menthol-glucuronide, was observed in the urine of smokers of either menthol or non-menthol cigarettes. The fact that a significant inverse correlation was observed between the levels of urinary menthol-glucuronide and NNAL-N-glucuronide, a major detoxification metabolite of the tobacco carcinogen, NNK, suggests that menthol may be inhibiting the clearance of this important tobacco carcinogen.

DMD Fast Forward. Published on October 2, 2019 as DOI: 10.1124/dmd.119.088351
This article has not been copyedited and formatted. The final version may differ from this version.

INTRODUCTION

Tobacco use is considered by the World Health Organization to be the leading cause of preventable premature death in adults worldwide (Saika and Machii, 2012). Tobacco specific nitrosamines (TSNAs) including (methylnitrosamino)-1-(3-pyridyl)-1-butanone (NNK) are among the most potent carcinogens found in both tobacco smoke and smokeless tobacco. NNK is rapidly metabolized in smokers by carbonyl reduction to both the (*R*)- and (*S*)- enantiomers of the equally potent carcinogen, 4-(methylnitrosamino-1-(3-pyridyl)-1-butanol (NNAL) (Nemzek et al., 1998). The glucuronidation of NNAL by the UDP glucuronosyltransferase (UGT) family of enzymes is considered to be an important mechanism for NNK detoxification (Upadhyaya et al., 1999), forming an *O*-glucuronide (*O*-Gluc) on the alcohol within the NNAL side chain or an *N*-glucuronide (*N*-Gluc) on the nitrogen of the NNAL pyridine ring. UGTs 1A9, 1A10, 2B7, and 2B17 have been shown to form NNAL-*O*-Gluc (2000; Wiener et al., 2004a; Balliet et al., 2010; Chung et al., 2013; Gruber et al., 2013; Wassenaar et al., 2015), with UGTs 2B7 and 2B17 primarily responsible for the stereo-specific formation of (*S*)-NNAL-*O*-Gluc and (*R*)-NNAL-*O*-Gluc, respectively (Kozlovich et al., 2015). While both UGTs 2B10 and 1A4 were shown to form NNAL-*N*-Gluc *in vitro* (Wiener et al., 2004a; Wiener et al., 2004b; Chen et al., 2008b; Kozlovich et al., 2015), UGT2B10 is responsible for >90% of NNAL-*N*-Gluc formation in human liver microsomes (HLM) and in the urine of smokers (Chen et al., 2008b; Chen et al., 2016; Murphy et al., 2018b).

Menthol is a flavor additive in many brands and types of tobacco products. It is listed by the FDA as ‘generally regarded as safe’ (GRAS) but is regulated as a drug when it is the active ingredient in a medication and subsequently has required dosage labeling in these situations. However, when used as a flavor additive in tobacco products, there are no labeling requirements for the amount of menthol added (Committee, 2011). While a cohort study

reported an increased risk of developing lung cancer for male menthol smokers when compared to non-menthol smokers (Sidney et al., 1995), other epidemiologic investigation have not found similar trends (Kabat and Hebert, 1991; Carpenter et al., 1999; Brooks et al., 2003; Stellman et al., 2003; Murray et al., 2007; Blot et al., 2011; Rostron, 2012; Munro et al., 2016). Indeed, epidemiology data from the entire Southern Community Cohort Study, from which the urine samples in the present analysis were drawn, show a significantly lower lung cancer risk, by about 30%, among menthol than non-menthol smokers for both black and white racial groups (Blot et al., 2011; Munro et al., 2016), and two meta analyses likewise show lower rather than higher risks of lung cancer among menthol compared to non-menthol smokers (Lee, 2011; Jones et al., 2013). However, with the presence of menthol in many edible and topical products in the U.S., the presence of either L- or D-menthol metabolites in the urine of smokers could be from menthol sources other than tobacco. Previously, urinary menthol was not previously found to be associated directly with levels of dietary menthol (Benowitz et al., 2010), and potentially could arise from a complex mix of exposures from edible, topical, and tobacco products in both menthol and non-menthol smokers. Since the underlying mechanism to determine menthol's impact for health risk in smokers is currently unknown, an understanding of the molecular basis of menthol clearance and the mechanism of inhibition within the clearance pathway of tobacco carcinogens may aid in understanding the health disparities for the racial groups with the highest rate of menthol cigarette use.

Menthol is a chiral aliphatic alcohol, existing as either the D- or L-menthol and the racemic mixture referred to as DL-menthol. The only naturally occurring enantiomer, the one found in and isolated from a variety of mint plant species, is L-menthol. The other enantiomer, D-menthol, is a product of the Haarmann & Reimer industrial synthesis process which yields a DL-menthol mixture (Oertling et al., 2007). It has been long known that D-menthol doesn't produce the same smell and taste profile normally associated with naturally occurring menthol

DMD Fast Forward. Published on October 2, 2019 as DOI: 10.1124/dmd.119.088351
This article has not been copyedited and formatted. The final version may differ from this version.

and that its analgesic properties are greatly reduced when compared to L-menthol (Eccles et al., 1988; Bhatia et al., 2008; Lawrence et al., 2011). When menthol is the active ingredient in over-the-counter pharmaceuticals, such as lozenges, only the L-menthol enantiomer tends to be present (Administration, 2018); however, the same may not be true for tobacco products (Committee, 2011). Studies have examined the total menthol content in both menthol and non-menthol cigarettes, which can range from 1.0 - 0.3% wt/wt with as low as 1.5 mg menthol per cigarette in menthol cigarettes (Celebucki et al., 2005), and up to 0.03% wt/wt with an upper level of 0.07 mg menthol/cigarette in non-menthol cigarettes (Giovino et al., 2004). While DL-menthol has previously been identified as an inhibitor of both NNAL-*O*-Gluc and NNAL-*N*-Gluc production in HLM (Muscat et al., 2009), no studies have been performed to determine which UGT enzymes are being inhibited or which menthol enantiomer is driving the inhibition.

The racial groups in the U.S. with the highest rate of menthol smokers, African Americans (Sidney et al., 1995) and Native Hawaiians (Committee, 2011), also have the highest rate of tobacco-related cancers among smokers (Coultas et al., 1994; Haiman et al., 2006; Daraei and Moore, 2015; Xie et al., 2017; Murphy et al., 2018a). It has been shown that while African Americans smoke fewer cigarettes per day than smokers in other racial groups (Caraballo et al., 1998; Benowitz et al., 2009; Benowitz et al., 2011), they may be exposed to more toxins per cigarette (Clark et al., 1996; Perez-Stable et al., 1998). Native Hawaiians have a higher rate of tobacco-related DNA damage when compared to Caucasian and Japanese Americans (Park et al., 2018). Genetic differences in the tobacco addiction pathway do not seem to account for the differences in cancer risk observed between these populations (Murphy et al., 2018a).

The underlying mechanism or interaction of menthol within the tobacco carcinogen pathway has yet to be fully elucidated. L-menthol exhibits inhibition of CYP2A6 and CYP2A13 carcinogen activation and nicotine metabolism (Kramlinger et al., 2012), but CYPs do not

directly metabolize menthol. It is known that menthol is rapidly cleared from the body as a menthol glucuronide [MG; (Kaffenberger and Doyle, 1990; Gelal et al., 1999)], the same clearance pathway as the TSNAs. Yet, no previous research has described the complete clearance pathway of menthol enantiomers. The goal of the present study was to identify the enzymes responsible for the metabolism of both L- and D-menthol to their respective glucuronides, as both could possibly be found in tobacco products (Committee, 2011), and to investigate the potential impact of each menthol enantiomer on NNAL glucuronide formation *in vivo*.

DMD Fast Forward. Published on October 2, 2019 as DOI: 10.1124/dmd.119.088351
This article has not been copyedited and formatted. The final version may differ from this version.

METHODS

Chemicals and materials. *rac*-NNAL (M325740), NNAL-*N*-Gluc (M325745), NNAL-*O*-Gluc (M325720), NNAL-$13C_6$ (M325741), L-MG (M218880), L-MG-d_4 (M218882) NNAL-*N*-Gluc-d_3 (M325747), NNAL-*O*-Gluc-d_5 (M325722), creatinine (C781500), and creatinine-d_3 (C781502) were purchased from Toronto Research Chemicals (Toronto, ON, Canada). L- and D-menthol (W266523, 224464), UDP glucuronic acid (UDPGA), alamethicin, methanol (MeOH) and acetonitrile (ACN) were purchased from Sigma (St Louis, MO). Dulbecco's modified Eagle's medium, fetal bovine serum (FBS), geneticin and penicillin-streptomycin were purchased from Life Technologies (Carlsbad, CA). The Pierce BCA protein assay kit, ammonium acetate and formic acid were purchased from Fisher Scientific (Fair Lawn, NJ).

Subjects and biospecimens. Urine and subject demographics were obtained from 100 self-identified current smokers upon recruitment into the Southern Community Cohort Study (SCCS), a prospective cohort of over 84,000 participants recruited between 2002-2009 (Signorello et al., 2010). One-time spot urine samples (~60 mL) were collected from SCCS participants at community health centers beginning in 2004. Samples were refrigerated on-site and shipped overnight to Vanderbilt Medical Center where urine was mixed with a small amount of ascorbic acid and stored at -80°C.

Urine specimens (150 µL each) were randomly chosen from 50 menthol smokers and 50 non-menthol smokers, were received at Washington State University College of Pharmacy and Pharmaceutical Sciences for analysis by overnight shipment, and subsequently stored at -80°C. Smoking preference for menthol cigarettes was self-identified at the time of urine sample collection. Subjects were 34% white, 60% black, 1% Hispanic, and 5% mixed race, and comprised 56% women.

DMD Fast Forward. Published on October 2, 2019 as DOI: 10.1124/dmd.119.088351
This article has not been copyedited and formatted. The final version may differ from this version.

Pooled (n=200) HLM and pooled (n=10) human intestinal microsomes (HIM) were purchased from Xenotech (Lenexa, KS).

Cell lines and microsomal preparation. Individual HEK293 cell lines overexpressing 18 human UGTs (1A1, 1A3, 1A4, 1A5, 1A6, 1A7, 1A8, 1A9, 1A10, 2A1, 2A2, 2A3, 2B4, 2B7, 2B10, 2B11, 2B15, and 2B17) have been described previously (Ren et al., 2000; Dellinger et al., 2006; Sun et al., 2006). The parent HEK293 cell line used in this study was obtained prior to 2000, and most recently authenticated by the American Type Culture Collection utilizing short tandem repeat (STR) analysis in December 2017. The individual HEK293 UGT overexpressing cell lines were verified to contain the UGT clone of interest by Sanger sequencing in August 2016 by Gene Wiz, LLC. All HEK293 cell lines were grown in 150 mm plates to 80% confluence in 30 mL of Dulbecco's modified Eagle's medium supplemented with 10% fetal bovine serum, and maintained in 400 µg/mL of geneticin in a humidified incubator atmosphere of 5% CO_2. For the preparation of cell microsomal fractions, cells were suspended in phosphate buffered saline (PBS) and subjected to five rounds of freeze/thaw before gentle homogenization. The cell homogenate was centrifuged at 9,000 *g* for 30 min at 4°C and the supernatant was further centrifuged at 105,000 *g* for 60 min at 4°C. The microsomal pellet was re-suspended in PBS and stored at -80°C. Total microsomal protein concentrations were determined using the BCA protein assay.

L- and D-menthol glucuronidation assay. L- and D-MG formation was determined in HLM (10 µg protein), HIM (20 µg protein), and UGT-expressing cell microsomes (15-20 µg protein) after pre-incubation with alamethicin (50 µg/mg protein; resulting in pores within the microsomal membrane) for 10 min on ice. Incubations (20 µL, final volume) included 50 mM Tris-HCl (pH 7.4), 10 mM $MgCl_2$, 4 mM UDPGA, 2% BSA, and either D- or L-menthol. Screening assays used 1.0 mM D- or L-menthol as substrate while kinetic analysis used a

DMD Fast Forward. Published on October 2, 2019 as DOI: 10.1124/dmd.119.088351
This article has not been copyedited and formatted. The final version may differ from this version.

range of 0.02-2.5 mM D- or L-menthol. Reactions were carried out at 37°C for 30 min and terminated by the addition of an equal volume of cold methanol and spiked with 2 µL of L-MG-d_4 (1 ppm). The precipitate was removed by centrifugation at 16,000 *g* for 10 min at 4°C and the supernatant was analyzed by liquid chromatography mass spectroscopy (LC-MS/MS) as described below. The rate of menthol glucuronidation was linear for up to 60 min. Each analysis was performed in triplicate.

NNAL-Gluc inhibition assay. L- and D-menthol inhibition of NNAL-Gluc formation in HLM and UGT-overexpressing cell microsomes was performed as described above using *rac*-NNAL (1 mM) as substrate and either the D- or L-menthol enantiomers (1.0-2,500 µM) as inhibitors. Reactions were performed at 37°C for 60 min, terminated by the addition of an equal volume of cold methanol, and spiked with 2 µL of NNAL-Gluc internal standard mix (NNAL-*N*-Gluc-d_3 and NNAL-*O*-Gluc-d_5, 2 ppm). Precipitate was removed by centrifugation at 16,000 *g* for 10 min at 4°C and the supernatant was analyzed by LC-MS/MS as described below. As described previously for *in vitro* NNAL glucuronidation assays, NNAL glucuronidation rates were linear for up to 2 h (Chen et al., 2008a). Each analysis was performed in triplicate.

LC-MS/MS analysis. For *in vitro* activity assays with HLM, HIM or HEK293 UGT-overexpressing cell microsomes, LC separation of NNAL metabolites was achieved using an Acquity H class ultra-performance liquid chromatography [UPLC; Waters, Milford, MA]. NNAL-Gluc peaks were analyzed essentially as described previously (Kozlovich et al., 2015), with a HSS T3 1.8 µm column (2.1x100 mm; Acquity, Waters) at 30°C by gradient elution at a flow rate of 0.35 mL/min using the following conditions: 0.5 min with 99% buffer A (5 mM ammonium formate with 0.01% formic acid) and 1% buffer B (100% MeOH), followed by a linear gradient for 3.0 min to 20% buffer B, and a subsequent linear gradient for 1.0 min to 95% buffer B. The

DMD Fast Forward. Published on October 2, 2019 as DOI: 10.1124/dmd.119.088351
This article has not been copyedited and formatted. The final version may differ from this version.

column was subsequently washed with a linear gradient to 1% buffer B for 1.0 min and re-equilibrated for 1.0 min in 1% buffer B.

MG peaks were analyzed using the same LC-MS/MS system with the column at 30°C with gradient elution at 0.30 mL/min using the following conditions: 0.5 min with 95% buffer A (5 mM ammonium acetate): 5% buffer B (100% acetonitrile), followed by a linear gradient for 9.5 min to 25% buffer A, and a subsequent linear gradient for 3 min to 5% buffer A. Equilibrium was re-established after a 1 min linear gradient to 95% buffer A.

The Waters Xevo TQD tandem mass spectrometer (MS) was equipped with a Zspray electrospray ionization interface operated in the positive ion mode for *in vitro* NNAL-Gluc detection, with capillary voltage at 0.6 kV. Nitrogen was used as both the cone gas and desolvation gas at 50 and 800 L/hr, respectively. Ultra-pure argon was used for collision-induced dissociation. The desolvation temperature and the ion source temperature were 500°C and 150°C, respectively. For the detection of NNAL glucuronides, the mass spectrometer was operated in the multiple reaction monitoring mode (MRM) with the following transitions: NNAL-*N*-Gluc, MS transition of 386.2 *m/z* >180.1 *m/z* with cone voltage and collision energy at 15 and 20 V, respectively; NNAL-*O*-Gluc, MS transition of 386.2 *m/z* >162.1 *m/z* with the cone voltage and collision energy each at 15 V.

MG detection was performed on the same Xevo TQD instrument with the electrospray interface operated in the negative ion mode with capillary voltage at 2.0 kV. Nitrogen was used as both the cone gas and desolvation gas at 50 and 800 L/h, respectively. Ultra-pure argon was used for collision-induced dissociation and the desolvation temperature and the ion source temperature were 500 and 150°C, respectively. For the detection of MG's, the mass spectrometer was operated in the MRM mode with a transition of 331.0 *m/z* >84.9 *m/z* with cone voltage and collision energy at 46 and 24 V, respectively.

For analysis of urine specimens, 2x 10 µl aliquots of each specimen were spiked with either 5 µl of an internal standard mixture that included NNAL-$13C_6$, NNAL-*N*-Gluc-$13C_6$ and

DMD Fast Forward. Published on October 2, 2019 as DOI: 10.1124/dmd.119.088351
This article has not been copyedited and formatted. The final version may differ from this version.

NNAL-*O*-Gluc-$13C_6$ (NNAL-Gluc-$13C_6$ was biosynthesized from NNAL-$13C_6$ using a previously published method (Chen et al., 2016); 0.1 ppm each), or 5 µL of L-MG-d_4 (3 ppm). After the addition of 10 µl of 0.5 M ammonium formate, the mixture was vortexed thoroughly. All precipitate was removed by centrifugation at 16,000 *g* for 10 min at 4°C. The supernatant was transferred into 350 µl conical glass sample vials for LC-MS/MS analysis. MG's were detected and quantified using the same LC-MS/MS methods described above. Urinary NNAL and its metabolites were detected and quantified with minor changes from a previously described method (Chen et al., 2016), using an Acquity UPLC with an HSS T3 (100 X 2.1 mm, 1.8 µm) UPLC column and a Xevo G2-S Qtof MS. The LC method was performed using a 5 µl sample injection volume, a 25°C column temperature and a flow rate of 0.20 mL/min using the following conditions: a 1 min linear gradient of 100% buffer A (5 mM ammonium formate with 0.01% formic acid) to 99% buffer A: 1% buffer B (100% acetonitrile), a subsequent isocratic gradient of 1% buffer B for 9 min, followed by a linear gradient for 8 min to 3% buffer B. After an 8 additional minutes at 3% buffer B, the column was cleaned with 95% buffer B and re-equilibrated to initial conditions before the next sample injection.

The Waters Xevo G2-S Qtof MS was operated in positive electrospray ionization MS/MS sensitive mode, with capillary voltage at 0.6 kV. Nitrogen was used for both cone and desolvation gases at 50 L/h and 800 L/h, respectively. Ultra-pure argon was used as the collision gas with a flow rate of 0.1 L/h for collision-induced dissociation. The source temperature was 120ºC, desolvation gas temperature was 500ºC. The dwell time for each ion was 0.1 sec. The cone voltage was 15, 25 and 15 V and the collision energies were 10, 20 and 15 volts for NNAL, NNAL-*N*-Gluc and NNAL-*O*-Gluc, respectively. The MS transition for quantification for NNAL-*N*-Gluc, NNAL-*O*-Gluc, NNAL and respective internal standards (IS) are 386.2>180.124 (IS: 392.2>186.144), 386.2>162.115 (IS: 392.2>168.135) and 210.1>180.124 (IS: 216.2 >186.144), respectively.

DMD Fast Forward. Published on October 2, 2019 as DOI: 10.1124/dmd.119.088351
This article has not been copyedited and formatted. The final version may differ from this version.

The MS transitions and LC retention times for each molecule were compared to purchased NNAL-*O*-Gluc, NNAL-*N*-Gluc, NNAL, and MG standards. The levels of NNAL-*O*-Gluc, NNAL-*N*-Gluc, free NNAL, and MG were quantified against a standard curve made from authenticated standards for NNAL-*O*-Gluc, NNAL-*N*-Gluc, free NNAL or MG of known quantity (Toronto Research Chemicals). Each NNAL and NNAL-Gluc standard curve was linear from 10 ppm to 0.005 ppm; MG standard curves were linear from 50 ppm to 0.005 ppm. Free NNAL and NNAL glucuronides were measured simultaneously, as were L- and D-MG, as described above.

Urinary creatinine levels were determined as previously described (Chen *et al*., 2016). Briefly, 2 µL of each urine specimen was diluted 1,000-fold in water, with 10 µL of the diluted sample mixed with 10 µL of 0.1 ppm for LC-MS/MS analysis using the same QToF LC-MS/MS system described above. The creatinine-d_3 internal standard was also mixed into urine prior to dilution before LC-MS/MS analysis for a set of five randomly-chosen urine specimens, and comparable results were obtained. The MS trace for quantification of creatinine is 114.06 (IS: 117.08), with a linear range of detection from 2 to 20,000 ppm.

A stable isotope dilution method was used for method validation and accuracy. The specificity of all LC-MS/MS methods were validated using positive and negative control samples as well as by comparing peaks with those observed for purchased standards and isotope-labeled internal standards. Linearity was validated by $r^2 > 0.997$ for all standard curves. Assay precision was validated by repeated (3 – 5 times) sample quantification, with a coefficient of variation (CV) less than 10%. Since isotope-labeled internal standards were utilized in all LC-MS/MS analysis, matrix effects on analyte quantification was minimal. For quantification of urinary MG, NNAL and NNAL-Gluc's, urine specimens were directly spiked with internal standard and then analyzed by LC-MS/MS without sample extraction. Therefore, recovery or dilution effects were not a concern. Analyte quantification was based on the ratio of signal peak area vs. the peak area of the internal standard. Range and median analyte levels were consistent with previous publications (Chen *et al.*, 2016; Benowitz *et al.*, 2010)

DMD Fast Forward. Published on October 2, 2019 as DOI: 10.1124/dmd.119.088351
This article has not been copyedited and formatted. The final version may differ from this version.

Statistical analysis. Kinetic and inhibition constants, non-parametric ANOVA (Kruskal-Wallis) with Dunn's post-test, Student's t-test, and Spearman correlations were determined using Prism version 7.0 (GraphPad Software, San Diego, CA).

DMD Fast Forward. Published on October 2, 2019 as DOI: 10.1124/dmd.119.088351
This article has not been copyedited and formatted. The final version may differ from this version.

RESULTS

In order to develop a separation and detection method for L- and D-MG, DL-menthol was incubated with HLM. As shown in Figure 1, efficient separation of D- and L-MG peaks was observed using the LC-MS/MS method described in this study. This method produced two distinct peaks: L-MG with a retention time of approximately 5.76 min and D-MG with a retention time of approximately 5.85 min (panel A). The L-MG peak was confirmed by comparison to commercial L-MG-d_4 internal standard (retention time = 5.75 min; panel B). While pure deuterated D-MG was not available as an internal standard, the second peak exhibited a different retention time with the same mass transition, suggesting that this peak corresponds to D-MG. The coefficient of variation for the detection of L-MG and/or D-MG from assays with DL-menthol, L-menthol, and D-menthol were 12%, 9%, and 15%, respectively.

To determine which UGTs form the glucuronide for either L- or D-menthol, 18 human UGTs were screened for glucuronidation activity using UGT-overexpressing cell microsomes. UGTs 1A9, 1A10, 2A1, 2A2, 2A3, 2B4, 2B7 and 2B17 exhibited detectable levels of glucuronidation activity for both menthol enantiomers (summarized in Supplemental Table S1). While UGT1A7 exhibited detectable glucuronidating activity for L-menthol, no detectable activity was observed for D-menthol for this enzyme. UGTs 1A1, 1A3, 1A4, 1A5, 1A6, 1A8, 2B10, 2B11 and 2B15 all exhibited no detectable activity for either menthol enantiomer. UGT2B7 exhibited the lowest apparent K_M (0.35 µM) for L-menthol, followed by UGT2B17 < UGT2A1 $\underset{\sim}{}$ UGT1A9 < UGT1A10 (Table 1 and Supplemental Figure S1). A similar pattern was observed for D-menthol, with UGTs 2B7 and 2A1 exhibiting the lowest apparent K_M values (0.33 and 0.37 µM, respectively), followed by UGT2B17 $\underset{\sim}{}$ UGT1A9 < UGT1A10. The apparent K_M values observed by kinetic analysis for active UGT-overexpressing cell microsomes ranged from 0.35 – 4.1 mM for L-menthol and 0.22 – 1.9 mM for D-menthol, and were comparable to that observed for HLM (0.89 and 0.54 mM for L- and D-menthol, respectively) and HIM (1.7 and 0.99 mM for L- and D-

DMD Fast Forward. Published on October 2, 2019 as DOI: 10.1124/dmd.119.088351
This article has not been copyedited and formatted. The final version may differ from this version.

menthol, respectively; Table 1). Kinetic parameters could not be obtained for UGTs 1A7, 2A2, 2A3, and 2B4 due to low overall activity. With the exception of UGT2B7, all of the UGTs as well as HLM and HIM exhibited higher turnover rates (V_{max}/K_M) for D-menthol than L-menthol (Table 1), suggesting that active UGTs have a higher clearance for D-menthol as a substrate. There was a 1,220- and 2,315-fold higher V_{max}/K_M observed for HLM than HIM for D- and L-menthol, respectively.

To determine the potential impact of menthol on the inhibition of NNAL glucuronidation, assays were initially performed with HLM, 1 mM *rac*-NNAL, and each menthol enantiomer ranging in concentration from 1.0 µM – 2.5 mM, with individual NNAL glucuronides detected by LC-MS/MS as described in the Materials and Methods. IC_{50} values were similar when inhibition assays were performed at either 30 min (data not shown) or 60 min. Both L- and D-menthol showed some level of inhibition for the formation of each NNAL glucuronide product in HLM, with the strongest inhibition exhibited for NNAL-*N*-Gluc formation (IC_{50} values of 100 µM and 50 µM, respectively; Table 2). The IC_{50} values were 6.6- and 13.8-fold higher for (*S*)-NNAL-*O*-Gluc vs. NNAL-*N*-Gluc formation, and 7.5- and 25.4-fold higher for (*R*)-NNAL-*O*-Gluc vs. NNAL-*N*-Gluc formation, for L- and D-menthol, respectively, in HLM. While the IC_{50} value was 2-fold higher for L- vs. D-menthol for NNAL-*N*-Gluc formation, D-menthol exhibited a 1.7-fold higher IC_{50} value as compared to L-menthol for (*R*)-NNAL-*O*-Gluc formation; no difference was observed between L- and D-menthol for the formation of (*S*)-NNAL-*O*-Gluc (IC_{50} values = 660 and 690 µM, respectively).

The formation of NNAL-*N*-Gluc by UGT2B10 was similarly inhibited by both L- and D-menthol (IC_{50} values = 236 and 202 µM, respectively); consistent with that observed in previous studies (Muscat et al., 2009), no NNAL-*N*-Gluc formation was detected for cell microsomes overexpressing UGTs 1A9, 1A10, 2B7 and 2B17 (with or without the addition of D- or L-menthol). The highest levels of inhibition of NNAL-*O*-Gluc formation by menthol enantiomers

DMD Fast Forward. Published on October 2, 2019 as DOI: 10.1124/dmd.119.088351
This article has not been copyedited and formatted. The final version may differ from this version.

was observed for UGT2B7 for (*S*)-NNAL-*O*-Gluc (IC_{50} values = 163 and 343 μM for L- and D-menthol, respectively). Less inhibition was observed for menthol enantiomers of UGT1A9- and UGT2B17-induced NNAL-*O*-Gluc formation; neither menthol enantiomer exhibited strong inhibition of the extra-hepatic UGT1A10.

To examine the potential effect of menthol inhibition on NNAL-Gluc formation *in vivo*, a panel of 100 urine specimens were examined from smokers recruited into the Southern Community Cohort Study. As shown in Table 3, 50% of the subjects indicated that they were smokers of mentholated cigarettes, with subjects smoking an average of 15 cigarettes/day. Each specimen was analyzed for levels of D-MG, L-MG, (*R*)-NNAL-*O*-Gluc, (*S*)-NNAL-*O*-Gluc, NNAL-*N*-Gluc, and free NNAL. MG was detected in all 50 menthol smokers and in 47 of the 50 non-menthol smokers. The fact that 3 of the non-menthol smokers exhibited no detectable level of MG suggested method specificity. Identification of the MG peak was verified by comparison to the retention time of the heavy isotope-labeled internal standard and a purchased analytical standard (Figure 1). Blank samples were analyzed by LC-MS/MS immediately after individual urine samples and showed no sample carry-over (data not shown). Total urinary MG levels ranged from 0 – 255 μg/mg creatinine. L-MG was the most prevalent menthol metabolite in these urine specimens (Figure 2, panel A). Urinary L-MG and D-MG were detected in 97 and 44 of the subjects, respectively, with L-MG detectable in specimens from 50 menthol smokers and 47 non-menthol smokers and D-MG detectable in 18 menthol smokers and 26 non-menthol smokers. In only 3 specimens from non-menthol smokers was no MG (L- or D-) detected. When detectable (n=44 specimens), urinary D-MG comprised an average of 2.8% of total MG. For the 97 specimens with detectable MG (either L- and/or D-menthol), D-menthol comprised an average of 1.3% of total MG. The range in the ratio of D-MG:total MG in the 44 specimens with detectable D-MG was 0.0010 - 0.20. No significant differences in MG levels were observed for specimens from smokers who self-reported being menthol vs. non-menthol smokers (Figure 2,

DMD Fast Forward. Published on October 2, 2019 as DOI: 10.1124/dmd.119.088351
This article has not been copyedited and formatted. The final version may differ from this version.

panel A). In addition, there were no significant differences in urinary MG levels between specimens from white vs. black menthol smokers (p=0.25) or white vs. black non-menthol smokers (p=0.51; data not shown). When stratifying specimens based on levels of total urinary MG (Figure 2, panel B), there were more specimens from non-menthol smokers vs. menthol smokers in the two lowest groups (0 - 5 and 6 - 10 µg MG/mg creatinine) but also in the highest group (76+ µg MG/mg creatinine). While the levels of MG in specimens from menthol smokers had a wider distribution, the curve was skewed to the lower MG levels, with a small number of specimens exhibiting high MG levels. A large gap in distribution was observed with no specimens within the MG levels ranging from 46 - 70 µg MG/mg creatinine.

To better assess the potential interaction between menthol and NNAL detoxification, NNAL and its glucuronides were measured in all 100 urine specimens (Table 4). NNAL metabolites were detectable in all of the urine specimens analyzed, with one specimen falling below the limit of quantification for (*R*)-NNAL-*O*-Gluc. The levels of total urinary NNAL were positively correlated with cigarettes per day (r = 0.4). There were no significant differences between specimens from white and black smokers for (*S*)-NNAL-*O*-Gluc (p=0.28), (*R*)-NNAL-*O*-Gluc (p=0.51), NNAL-*N*-Gluc (p=0.82), or free NNAL (p=0.77), suggesting that race was not a factor when assessing the levels of these urinary metabolites. The levels of each urinary metabolite (MG, free NNAL, and each NNAL-Gluc) were similar between smokers of menthol and non-menthol branded cigarettes (Table 5). No significant correlations were observed for any of the urinary NNAL glucuronides (or for free NNAL) when compared with total urinary MG in the 100 specimens (Spearman coefficient test; data not shown). No significant difference was observed in the levels of free NNAL between MG tertile groups when examining free NNAL alone (Supplemental Table S2) or as a ratio with total NNAL (results not shown). To normalize individual NNAL metabolite levels between individuals, each of the urinary NNAL-Gluc's were determined as a ratio with free NNAL as the denominator. When specimens were stratified by tertiles based on levels of total urinary MG (termed 'low', 'intermediate' and 'high'), significantly

DMD Fast Forward. Published on October 2, 2019 as DOI: 10.1124/dmd.119.088351
This article has not been copyedited and formatted. The final version may differ from this version.

lower levels of urinary NNAL-*N*-Gluc (as a ratio with free NNAL) was observed in both the intermediate ($p<0.01$) and high ($p<0.05$) urinary MG groups as compared to the low urinary MG group (Figure 3). Specimens with intermediate and high urinary MG levels exhibited similar NNAL-*N*-Gluc levels. While a trend towards lower (R)-NNAL-O-Gluc levels were also observed in the higher MG tertile groups, these differences were not significant (Figure 3). No significant difference was observed for (*S*)-NNAL-*O*-Gluc between different urinary MG groups. No significant differences in the levels of any of the NNAL-Gluc's were observed when using total NNAL as the denominator (results not shown).

DMD Fast Forward. Published on October 2, 2019 as DOI: 10.1124/dmd.119.088351
This article has not been copyedited and formatted. The final version may differ from this version.

DISCUSSION

In the present study, the metabolism of menthol was explored by utilizing a panel of 18 human UGTs that were screened for MG formation activity. UGTs 1A9, 1A10, 2A1, 2B7, and 2B17 all exhibited relatively high glucuronidation affinity for both L- and D-menthol, with K_M values that were similar to those observed in HLM and HIM. The activity observed for UGT2B7 in the present study (K_M = 0.35 μM) is consistent with that observed previously for UGT2B7 against L-menthol (Bhasker et al., 2000). The fact that UGT1A3 exhibited no activity against menthol enantiomers in the present study is also consistent with the lack of activity against menthol shown in previous studies (Green and Tephly, 1996). UGTs 2A1 and 1A10 are extra-hepatic enzymes that are expressed in digestive tract tissues (Zheng et al., 2002; Dellinger et al., 2006; Bushey et al., 2011) and are likely contributing to the MG formation observed in HIM. UGTs 1A9, 2B7, and 2B17 are hepatically-expressed enzymes (Zheng et al., 2002; Jones and Lazarus, 2014) that could all be playing a role in MG formation in HLM. UGTs 2A1 and 2B7 exhibited the highest affinity for D-menthol while UGTs 2B7 and 2B17 exhibited the highest affinity for L-menthol. While previous studies suggested that UGT1A4 exhibited glucuronidation activity against menthol enantiomers (Green and Tephly, 1996), no detectable activity was observed for this enzyme in the current study. This difference in activity may be due to differences in assay sensitivity between studies.

Racemic, DL-menthol was previously shown to inhibit the formation of both NNAL-*N*-Gluc and NNAL-*O*-Gluc formation in HLM (Muscat et al., 2009). NNAL-*O*-Gluc formation is catalyzed by several of the same UGTs [1A9, 1A10, 2B7, and 2B17; (Balliet et al., 2010; Kozlovich et al., 2015; Kozlovich et al., 2019)] that are also most active against menthol enantiomers. In the current study, the individual L- and D-menthol enantiomers were further studied as potential inhibitors of these UGTs as well as UGT2B10, which is known to be the

primary enzyme involved in NNAL-*N*-Gluc formation (Chen et al., 2008b; Kozlovich et al., 2015; Chen et al., 2016) and is expressed in several tobacco-related cancer tissues (Jones and Lazarus, 2014; Kozlovich et al., 2019). While L- and D-menthol exhibited the strongest inhibition potential for formation of NNAL-*N*-Gluc in HLM, each enantiomer also exhibited some level of inhibition for HLM formation of (*R*)- and (*S*)-NNAL-*O*-Gluc. When each UGT enzyme was individually assayed for inhibition, both menthol enantiomers exhibited high inhibition potential for UGT2B7-mediated formation of (*S*)-NNAL-*O*-Gluc. These data are similar to other studies where menthol and other mercaptoid alcohols have been associated with the inhibition of UGT2B7 activity (Ishii et al., 2012). A similarly high inhibition potential was observed for UGT2B10-mediated formation of NNAL-*N*-Gluc. This inhibition of the hepatically-expressed UGT2B7 and UGT2B10 is consistent with the inhibition of NNAL-*O*-Gluc and NNAL-*N*-Gluc observed previously in HLM (Muscat et al., 2009).

Many studies have examined menthol vs non-menthol smokers in an attempt to determine the impact of menthol on tobacco-related diseases, with several studies measuring MG as a potential biomarker for identification of menthol or non-menthol cigarettes smokers. For example, one study indicated that the levels of urinary menthol (measured as MG) were not correlated with the use of menthol vs non-menthol cigarettes (Benowitz et al., 2010), while another study found significantly higher MG levels in the blood of menthol vs non-menthol smokers (Hsu et al., 2017). Consistent with these studies, results from the present study indicated that the levels of urinary MG were not correlated with subjects self-identifying as menthol or non-menthol cigarette smokers. These studies are consistent with the hypothesis that menthol branding is not an accurate method of examining the effects of menthol on tobacco-induced diseases.

The analysis of potential menthol-induced inhibition of NNAL-Gluc formation *in vivo* was performed in the present study by stratifying smokers into groups based on quantified levels of

DMD Fast Forward. Published on October 2, 2019 as DOI: 10.1124/dmd.119.088351
This article has not been copyedited and formatted. The final version may differ from this version.

urinary MG rather than by menthol vs non-menthol cigarette branding type. Interestingly, the levels of urinary D-MG were relatively low as compared to the levels of urinary L-menthol, comprising, on average, 1.3% of the total menthol exposure for specimens from smokers with detectable urinary menthol. The group with the lowest urinary MG levels exhibited the highest levels of urinary NNAL-*N*-Gluc, suggesting a potential interaction between menthol and NNAL-*N*-Gluc formation, likely mediated by UGT2B10 based on the inhibition of UGT2B10 by menthol enantiomers *in vitro*. These data are consistent with the inhibitory effects observed with DL-menthol in HLM in previous studies (Muscat et al., 2009). A similar but non-significant trend was observed for (*R*)-NNAL-*O*-Gluc formation, an effect potentially due to menthol inhibition of the (*R*)-NNAL-*O*-Gluc forming enzyme, UGT2B17. A possible confounder was that UGT2B17, which plays an important role in (*R*)-NNAL-*O*-Gluc formation (Kozlovich et al., 2015; Chen et al., 2016), has a prevalent copy number variant [minor allele frequency = 0.30 in Caucasians (Geer et al., 2010)] that was not examined in this population. To better examine the potential inhibitory effects of menthol on (*R*)-NNAL-*O*-Gluc formation, a larger smoking population will be required.

Interestingly, the inhibition of (*S*)-NNAL-*O*-Gluc formation was observed for menthol enantiomers using UGT2B7-expressed cell microsomes in the current study. While this could in part be due to the large variability in (*S*)-NNAL-*O*-Gluc formation observed between subjects, it is also likely that, consistent with other studies (Kozlovich et al., 2015; Chen et al., 2016), other UGTs involved in (*S*)-NNAL-*O*-Gluc formation that are not as inhibited by menthol, including UGT1A9, may be important in hepatic (*S*)-NNAL-*O*-Gluc formation in addition to UGT2B7. While a trend towards lower (R)-NNAL-O-Gluc levels were also observed in the higher MG tertile groups in the present study, these differences were not significant, suggesting that larger studies will be required to fully examine this potential effect.

While at lower levels than in menthol-branded cigarettes, menthol is also present in cigarettes classified as ‘non-menthol’ (Committee, 2011). The levels of menthol in non-menthol

cigarettes may still be at levels which could inhibit NNAL detoxification, especially in cases where the levels of menthol in non-menthol cigarettes still far exceed the levels of NNK per cigarette. Non-menthol cigarettes can contain up to 0.07 mg menthol per cigarette (Ai et al., 2016) while NNK levels are over 10-fold lower (Ding et al., 2008; Rickert et al., 2008). Therefore, menthol content in non-menthol cigarettes could have been important confounders in previous epidemiologic studies examining the role of menthol as a factor in lung cancer risk (comparing 'menthol' vs 'non-menthol' smokers). However, menthol is an additive in many edible and topical products and may have been consumed by some of the non-menthol (as well as menthol) cigarette smoking subjects for whom urines were analyzed in this study, potentially affecting the levels of urinary MG detected in these subjects. A confounder when considering edible menthol products as an inhibitor of NNAL metabolism is the potential for differential glucuronidation of menthol by extra-hepatic UGTs that are expressed in the digestive tract (i.e., UGTs 1A7, 1A8, 1A10). Limitations of the present study include the fact that no information regarding very recent menthol consumption or exposure from other sources was collected from recruited subjects at the time of urine collection. Additionally, there could be racial and/or gender variation in creatinine formation; the sample size used in the present study was not large enough to separate by either race or gender.

In summary, both menthol and NNAL are metabolized by some of the same UGT enzymes. Higher levels of urinary MG were shown to be correlated with decreases in urinary NNAL-*N*-Gluc in smokers, suggesting that the presence of menthol could potentially lead to NNAL being metabolized by different metabolic pathways, which could subsequently increase the opportunity for NNAL to result in increased DNA damage and increase the potential of tobacco-related cancers. The data presented in this study suggests that additional studies are required to better delineate the relationship between menthol, tobacco carcinogen detoxification, and cancer risk.

DMD Fast Forward. Published on October 2, 2019 as DOI: 10.1124/dmd.119.088351
This article has not been copyedited and formatted. The final version may differ from this version.

Acknowledgements

The authors thank the Mass Spectrometry Core facility at Washington State University (WSU) Spokane for their help with LC-MS/MS.

Author Contributions

Participated in research design: Kozlovich, Watson, Chen, and Lazarus.

Conducted experiments: Kozlovich, Watson, and Chen.

Contributed new reagents or analytic tools: Kozlovich, Chen, and Lazarus.

Performed data analysis: Kozlovich, Watson, Chen, and Lazarus.

Wrote or contributed to the writing of the manuscript: Kozlovich, Watson, Chen, and Lazarus.

REFERENCES

(2000) Obesity: preventing and managing the global epidemic. Report of a WHO consultation. *World Health Organ Tech Rep Ser* **894:**i-xii, 1-253.

Administration FaD (2018) Drugs for Human Use (Services DoHaH ed.

Ai J, Taylor KM, Lisko JG, Tran H, Watson CH, and Holman MR (2016) Menthol Content in US Marketed Cigarettes. *Nicotine Tob Res* **18:**1575-1580.

Balliet RM, Chen G, Dellinger RW, and Lazarus P (2010) UDP-glucuronosyltransferase 1A10: activity against the tobacco-specific nitrosamine, 4-(methylnitrosamino)-1-(3-pyridyl)-1-butanol, and a potential role for a novel UGT1A10 promoter deletion polymorphism in cancer susceptibility. *Drug Metab Dispos* **38:**484-490.

Benowitz NL, Bernert JT, Caraballo RS, Holiday DB, and Wang J (2009) Optimal serum cotinine levels for distinguishing cigarette smokers and nonsmokers within different racial/ethnic groups in the United States between 1999 and 2004. *Am J Epidemiol* **169:**236-248.

Benowitz NL, Dains KM, Dempsey D, Havel C, Wilson M, and Jacob P, 3rd (2010) Urine menthol as a biomarker of mentholated cigarette smoking. *Cancer Epidemiol Biomarkers Prev* **19:**3013-3019.

Benowitz NL, Dains KM, Dempsey D, Wilson M, and Jacob P (2011) Racial differences in the relationship between number of cigarettes smoked and nicotine and carcinogen exposure. *Nicotine Tob Res* **13:**772-783.

Bhasker CR, McKinnon W, Stone A, Lo AC, Kubota T, Ishizaki T, and Miners JO (2000) Genetic polymorphism of UDP-glucuronosyltransferase 2B7 (UGT2B7) at amino acid 268: ethnic diversity of alleles and potential clinical significance. *Pharmacogenetics* **10:**679-685.

Bhatia SP, McGinty D, Letizia CS, and Api AM (2008) Fragrance material review on d-menthol. *Food Chem Toxicol* **46 Suppl 11:**S215-217.

Blot WJ, Cohen SS, Aldrich M, McLaughlin JK, Hargreaves MK, and Signorello LB (2011) Lung cancer risk among smokers of menthol cigarettes. *J Natl Cancer Inst* **103:**810-816.

Brooks DR, Palmer JR, Strom BL, and Rosenberg L (2003) Menthol cigarettes and risk of lung cancer. *Am J Epidemiol* **158:**609-616; discussion 617-620.

Bushey RT, Chen G, Blevins-Primeau AS, Krzeminski J, Amin S, and Lazarus P (2011) Characterization of UDP-glucuronosyltransferase 2A1 (UGT2A1) variants and their potential role in tobacco carcinogenesis. *Pharmacogenet Genomics* **21:**55-65.

Caraballo RS, Giovino GA, Pechacek TF, Mowery PD, Richter PA, Strauss WJ, Sharp DJ, Eriksen MP, Pirkle JL, and Maurer KR (1998) Racial and ethnic differences in serum cotinine levels of cigarette smokers: Third National Health and Nutrition Examination Survey, 1988-1991. *JAMA* **280:**135-139.

Carpenter CL, Jarvik ME, Morgenstern H, McCarthy WJ, and London SJ (1999) Mentholated cigarette smoking and lung-cancer risk. *Ann Epidemiol* **9:**114-120.

Celebucki CC, Wayne GF, Connolly GN, Pankow JF, and Chang EI (2005) Characterization of measured menthol in 48 U.S. cigarette sub-brands. *Nicotine Tob Res* **7:**523-531.

Chen G, Dellinger RW, Gallagher CJ, Sun D, and Lazarus P (2008a) Identification of a prevalent functional missense polymorphism in the UGT2B10 gene and its association with UGT2B10 inactivation against tobacco-specific nitrosamines. *Pharmacogenet Genomics* **18:**181-191.

Chen G, Dellinger RW, Sun D, Spratt TE, and Lazarus P (2008b) Glucuronidation of tobacco-specific nitrosamines by UGT2B10. *Drug Metab Dispos* **36:**824-830.

Chen G, Luo S, Kozlovich S, and Lazarus P (2016) Association between Glucuronidation Genotypes and Urinary NNAL Metabolic Phenotypes in Smokers. *Cancer Epidemiol Biomarkers Prev* **25:**1175-1184.

Chung CJ, Pu YS, Shiue HS, Lee HL, Lin P, Yang HY, Su CT, and Hsueh YM (2013) 4-(Methylnitrosamino)-1-(3-pyridyl)-1-butanone (NNK) metabolism-related enzymes gene polymorphisms, NNK metabolites levels and urothelial carcinoma. *Toxicol Lett* **216:**16-22.

Clark PI, Gautam S, and Gerson LW (1996) Effect of menthol cigarettes on biochemical markers of smoke exposure among black and white smokers. *Chest* **110:**1194-1198.

Committee TPSA (2011) Menthol Cigarettes and Public Health: Review of the Scientific Evidence and Reccomendations. *Government Document Submitted to FDA*.

Coultas DB, Gong H, Jr., Grad R, Handler A, McCurdy SA, Player R, Rhoades ER, Samet JM, Thomas A, and Westley M (1994) Respiratory diseases in minorities of the United States. *Am J Respir Crit Care Med* **149:**S93-131.

Daraei P and Moore CE (2015) Racial Disparity Among the Head and Neck Cancer Population. *J Cancer Educ* **30:**546-551.

Dellinger RW, Fang JL, Chen G, Weinberg R, and Lazarus P (2006) Importance of UDP-glucuronosyltransferase 1A10 (UGT1A10) in the detoxification of polycyclic aromatic hydrocarbons: decreased glucuronidative activity of the UGT1A10139Lys isoform. *Drug Metab Dispos* **34:**943-949.

Ding YS, Zhang L, Jain RB, Jain N, Wang RY, Ashley DL, and Watson CH (2008) Levels of tobacco-specific nitrosamines and polycyclic aromatic hydrocarbons in mainstream smoke from different tobacco varieties. *Cancer Epidemiol Biomarkers Prev* **17:**3366-3371.

Eccles R, Griffiths DH, Newton CG, and Tolley NS (1988) The effects of D and L isomers of menthol upon nasal sensation of airflow. *J Laryngol Otol* **102:**506-508.

Geer LY, Marchler-Bauer A, Geer RC, Han L, He J, He S, Liu C, Shi W, and Bryant SH (2010) The NCBI BioSystems database. *Nucleic Acids Res* **38:**D492-496.

Gelal A, Jacob P, 3rd, Yu L, and Benowitz NL (1999) Disposition kinetics and effects of menthol. *Clin Pharmacol Ther* **66:**128-135.

Giovino GA, Sidney S, Gfroerer JC, O'Malley PM, Allen JA, Richter PA, and Cummings KM (2004) Epidemiology of menthol cigarette use. *Nicotine Tob Res* **6 Suppl 1:**S67-81.

Green MD and Tephly TR (1996) Glucuronidation of amines and hydroxylated xenobiotics and endobiotics catalyzed by expressed human UGT1.4 protein. *Drug Metab Dispos* **24:**356-363.

Gruber M, Le T, Filipits M, Gsur A, Mannhalter C, Jager U, and Vanura K (2013) UDP-glucuronosyltransferase 2B17 genotype and the risk of lung cancer among Austrian Caucasians. *Cancer Epidemiol* **37:**625-628.

Haiman CA, Stram DO, Wilkens LR, Pike MC, Kolonel LN, Henderson BE, and Le Marchand L (2006) Ethnic and racial differences in the smoking-related risk of lung cancer. *N Engl J Med* **354:**333-342.

Hsu PC, Lan RS, Brasky TM, Marian C, Cheema AK, Ressom HW, Loffredo CA, Pickworth WB, and Shields PG (2017) Metabolomic profiles of current cigarette smokers. *Mol Carcinog* **56:**594-606.

Ishii Y, Iida N, Miyauchi Y, Mackenzie PI, and Yamada H (2012) Inhibition of morphine glucuronidation in the liver microsomes of rats and humans by monoterpenoid alcohols. *Biol Pharm Bull* **35:**1811-1817.

Jones MR, Tellez-Plaza M, and Navas-Acien A (2013) Smoking, menthol cigarettes and all-cause, cancer and cardiovascular mortality: evidence from the National Health and Nutrition Examination Survey (NHANES) and a meta-analysis. *PLoS One* **8:**e77941.

Jones NR and Lazarus P (2014) UGT2B gene expression analysis in multiple tobacco carcinogen-targeted tissues. *Drug Metab Dispos* **42:**529-536.

Kabat GC and Hebert JR (1991) Use of mentholated cigarettes and lung cancer risk. *Cancer Res* **51:**6510-6513.

Kaffenberger RM and Doyle MJ (1990) Determination of menthol and menthol glucuronide in human urine by gas chromatography using an enzyme-sensitive internal standard and flame ionization detection. *J Chromatogr* **527:**59-66.

Kozlovich S, Chen G, and Lazarus P (2015) Stereospecific Metabolism of the Tobacco-Specific Nitrosamine, NNAL. *Chem Res Toxicol*.

Kozlovich S, Chen G, Watson CJ, and Lazarus P (2019) Prominent Stereo-selectivity of NNAL Glucuronidation in Upper Aerodigestive Tract Tissues. *Chem Res Toxicol*.

Kramlinger VM, von Weymarn LB, and Murphy SE (2012) Inhibition and inactivation of cytochrome P450 2A6 and cytochrome P450 2A13 by menthofuran, beta-nicotyrine and menthol. *Chem Biol Interact* **197:**87-92.

Lawrence D, Cadman B, and Hoffman AC (2011) Sensory properties of menthol and smoking topography. *Tob Induc Dis* **9 Suppl 1:**S3.

Lee PN (2011) Systematic review of the epidemiological evidence comparing lung cancer risk in smokers of mentholated and unmentholated cigarettes. *BMC Pulm Med* **11:**18.

Munro HM, Tarone RE, Wang TJ, and Blot WJ (2016) Menthol and Nonmenthol Cigarette Smoking: All-Cause Deaths, Cardiovascular Disease Deaths, and Other Causes of Death Among Blacks and Whites. *Circulation* **133:**1861-1866.

Murphy SE, Park SL, Balbo S, Haiman CA, Hatsukami DK, Patel Y, Peterson LA, Stepanov I, Stram DO, Tretyakova N, Hecht SS, and Le Marchand L (2018a) Tobacco biomarkers and genetic/epigenetic analysis to investigate ethnic/racial differences in lung cancer risk among smokers. *NPJ Precis Oncol* **2:**17.

Murphy SE, von Weymarn LB, Parenteau M, Stepanov I, Tiirikainen M, LeMarchand L, and Park SL (2018b) Influence of UGT2B10 Genotype on Urinary Excretion of 4-(Methylnitrosamino)-1-(3-pyridyl)-1-butanol- N-glucuronide by African American Smokers. *Chem Res Toxicol* **31:**168-175.

Murray RP, Connett JE, Skeans MA, and Tashkin DP (2007) Menthol cigarettes and health risks in Lung Health Study data. *Nicotine Tob Res* **9:**101-107.

Muscat JE, Chen G, Knipe A, Stellman SD, Lazarus P, and Richie JP, Jr. (2009) Effects of menthol on tobacco smoke exposure, nicotine dependence, and NNAL glucuronidation. *Cancer Epidemiol Biomarkers Prev* **18:**35-41.

Nemzek WR, Hecht S, Gandour-Edwards R, Donald P, and McKennan K (1998) Perineural spread of head and neck tumors: how accurate is MR imaging? *AJNR Am J Neuroradiol* **19:**701-706.

Oertling H, Reckziegel A, Surburg H, and Bertram HJ (2007) Applications of menthol in synthetic chemistry. *Chem Rev* **107:**2136-2164.

Park SL, Patel YM, Loo LWM, Mullen DJ, Offringa IA, Maunakea A, Stram DO, Siegmund K, Murphy SE, Tiirikainen M, and Le Marchand L (2018) Association of internal smoking dose with blood DNA methylation in three racial/ethnic populations. *Clin Epigenetics* **10:**110.

Perez-Stable EJ, Herrera B, Jacob P, 3rd, and Benowitz NL (1998) Nicotine metabolism and intake in black and white smokers. *JAMA* **280:**152-156.

Ren Q, Murphy SE, Zheng Z, and Lazarus P (2000) O-Glucuronidation of the lung carcinogen 4-(methylnitrosamino)-1- (3-pyridyl)-1-butanol (NNAL) by human UDP-glucuronosyltransferases 2B7 and 1A9. *Drug Metab Dispos* **28:**1352-1360.

Rickert WS, Joza PJ, Sharifi M, Wu J, and Lauterbach JH (2008) Reductions in the tobacco specific nitrosamine (TSNA) content of tobaccos taken from commercial Canadian cigarettes and corresponding reductions in TSNA deliveries in mainstream smoke from such cigarettes. *Regul Toxicol Pharmacol* **51:**306-310.

Rostron B (2012) Lung cancer mortality risk for U.S. menthol cigarette smokers. *Nicotine Tob Res* **14:**1140-1144.

Saika K and Machii R (2012) Cancer mortality attributable to tobacco by region based on the WHO Global Report. *Jpn J Clin Oncol* **42:**771-772.

Sidney S, Tekawa IS, Friedman GD, Sadler MC, and Tashkin DP (1995) Mentholated cigarette use and lung cancer. *Arch Intern Med* **155:**727-732.

Signorello LB, Hargreaves MK, and Blot WJ (2010) The Southern Community Cohort Study: investigating health disparities. *J Health Care Poor Underserved* **21:**26-37.

Stellman SD, Chen Y, Muscat JE, Djordjevic MV, Richie JP, Jr., Lazarus P, Thompson S, Altorki N, Berwick M, Citron ML, Harlap S, Kaur TB, Neugut AI, Olson S, Travaline JM, Witorsch P, and Zhang ZF (2003) Lung cancer risk in white and black Americans. *Ann Epidemiol* **13:**294-302.

Sun D, Chen G, Dellinger RW, Duncan K, Fang JL, and Lazarus P (2006) Characterization of tamoxifen and 4-hydroxytamoxifen glucuronidation by human UGT1A4 variants. *Breast Cancer Res* **8:**R50.

Upadhyaya P, Kenney PM, Hochalter JB, Wang M, and Hecht SS (1999) Tumorigenicity and metabolism of 4-(methylnitrosamino)-1-(3-pyridyl)-1-butanol enantiomers and metabolites in the A/J mouse. *Carcinogenesis* **20:**1577-1582.

Wassenaar CA, Conti DV, Das S, Chen P, Cook EH, Ratain MJ, Benowitz NL, and Tyndale RF (2015) UGT1A and UGT2B genetic variation alters nicotine and nitrosamine glucuronidation in european and african american smokers. *Cancer Epidemiol Biomarkers Prev* **24:**94-104.

Wiener D, Doerge DR, Fang JL, Upadhyaya P, and Lazarus P (2004a) Characterization of N-glucuronidation of the lung carcinogen 4-(methylnitrosamino)-1-(3-pyridyl)-1-butanol (NNAL) in human liver: importance of UDP-glucuronosyltransferase 1A4. *Drug Metab Dispos* **32:**72-79.

Wiener D, Fang JL, Dossett N, and Lazarus P (2004b) Correlation between UDP-glucuronosyltransferase genotypes and 4-(methylnitrosamino)-1-(3-pyridyl)-1-butanone glucuronidation phenotype in human liver microsomes. *Cancer Res* **64:**1190-1196.

Xie SH, Rabbani S, Petrick JL, Cook MB, and Lagergren J (2017) Racial and Ethnic Disparities in the Incidence of Esophageal Cancer in the United States, 1992-2013. *Am J Epidemiol* **186:**1341-1351.

Zheng Z, Fang JL, and Lazarus P (2002) Glucuronidation: an important mechanism for detoxification of benzo[a]pyrene metabolites in aerodigestive tract tissues. *Drug Metab Dispos* **30:**397-403.

Footnotes

a) These studies were funded in part by the National Institutes of Health, National Institutes of Environmental Health Sciences [Grant R01-ES025460] to P. Lazarus and the Health Sciences and Services Authority of Spokane, WA [Grant WSU002292] to Washington State University. The Southern Community Cohort Study was supported by the National Cancer Institute (grants R01CA092447 and U01CA202979). Data collection was performed by the Survey and Biospecimen Shared Resource which is supported in part by the Vanderbilt-Ingram Cancer Center (P30 CA68485).

b) The data contained in this manuscript were presented in whole or part at the Experimental Biology (2019) and Society for Research on Nicotine and Tobacco (2019) conferences, and as a chapter in the Doctoral Dissertation of Shannon Kozlovich.

Table 1. Kinetics for L- and D-menthol with UGT-expressing HEK293 cell lines.[a,b]

	L-menthol			D-menthol		
Enzyme	K_M (mM)	V_{max}[c] (pmol·mg protein^{-1}·min^{-1})	V_{max}/K_M[c] (nL·mg protein^{-1}·min^{-1})	K_M (mM)	V_{max}[c] (pmol·mg protein^{-1}·min^{-1})	V_{max}/K_M[c] (nL·mg protein^{-1}·min^{-1})
UGT1A9	2.1 ± 2.0	3.1 ± 2.2	1.7	0.80 ± 0.43	8.6 ± 2.3	12
UGT1A10	4.1 ± 0.9	16 ± 3.3	3.9	1.9 ± 1.2	16 ± 7.0	8.9
UGT2A1	1.8 ± 0.9	28 ± 7.2	16	0.37 ± 0.12	42 ± 3.6	120
UGT2B7	0.35 ± 0.03	54 ± 6.2	155	0.33 ± 0.12	48 ± 7.5	154
UGT2B17	0.70 ± 0.24	4.0 ± 1.3	5.9	0.76 ± 0.09	10 ± 1.7	14
HLM	0.89 ± 0.13	4167 ± 326	4802	0.54 ± 0.22	2805 ± 293	5721
HIM	1.7 ± 1.1	1.8 ± 0.90	1.1	0.99 ± 0.18	2.3 ± 0.25	2.3

[a] Data are expressed as the mean ± S.D. of three independent experiments.
[b] Seventeen human UGTs were screened for L- and D-menthol activity. UGTs 1A1, 1A3, 1A4, 1A5, 1A6, 1A8, 2B10 and 2B11 exhibited no activity when incubated with either L- or D-menthol. While UGTs 2A2, 2A3, and 2B4 exhibited glucuronidation activity against menthol enantiomers, it was too low to determine enzyme kinetics for both L- and D-menthol; UGT1A7 exhibited no detectible activity for D-menthol and its L-menthol glucuronidation activity was too low to determine enzyme kinetics.
[c] Units are expressed per mg total microsomal protein.

DMD Fast Forward. Published on October 2, 2019 as DOI: 10.1124/dmd.119.088351
This article has not been copyedited and formatted. The final version may differ from this version.

Table 2. L- and D-menthol inhibition constants (IC_{50}) for HLM and UGT-expressing cell microsomes for NNAL glucuronide formation.[a]

		NNAL-*N*-Gluc (μM)	**(*R*)-NNAL-*O*-Gluc** (μM)	**(*S*)-NNAL-*O*-Gluc** (μM)
L-menthol	HLM	100	750	660
	UGT1A9	NA[b]	632	689
	UGT1A10	NA	2309	>2500
	UGT2B7	NA	NA	163
	UGT2B10	236	NA	NA
	UGT2B17	NA	927	NA
D-menthol	HLM	50	1,265	690
	UGT1A9	NA	1480	1215
	UGT1A10	NA	1419	>2500
	UGT2B7	NA	NA	343
	UGT2B10	202	NA	NA
	UGT2B17	NA	995	NA

[a] Data are expressed as the mean of three independent experiments.
[b] NA, not applicable (reaction not expected to produce the product).

DMD Fast Forward. Published on October 2, 2019 as DOI: 10.1124/dmd.119.088351
This article has not been copyedited and formatted. The final version may differ from this version.

Table 3. Study subject demographics.

	all subjects (n=100)	**non-menthol smokers (n=50)**	**menthol smokers N=50**
Age, mean	49 y	52 y	47 y
Age, range	40-66 y	40–66 y	40–61 y
Sex	56% female	58% female	54% female
Race/ethnicity	34% white	62% white	6% white
	60% black	28% black	92% black
	1% Hispanic		2% Hispanic
	5% mixed race	10% mixed race	
Cig per day, mean (range)	15 (3-40)	20 (5-40)	11 (3-30)
Pack years, mean (range)	25 (1-98)	35 (6-98)	15 (1-41)

DMD Fast Forward. Published on October 2, 2019 as DOI: 10.1124/dmd.119.088351
This article has not been copyedited and formatted. The final version may differ from this version.

Table 4. Urinary NNAL and NNAL glucuronide levels in smokers by race.[a]

	ng/mg creatinine			
	(*S*)-NNAL-*O*-Gluc	(*R*)-NNAL-*O*-Gluc	NNAL-*N*-Gluc	free NNAL
		White Smokers		
mean	0.64 ± 0.062	0.18 ± 0.020	0.29 ± 0.026	0.16 ± 0.019
range	0.074-1.66	0.22-0.47	0.076-0.69	0.050-0.51
		Black Smokers		
mean	0.54 ± 0.15	0.16 ± 0.053	0.30 ± 0.14	0.21 ± 0.092
range	0.051-8.90	0-3.2	0.017-8.5	0.009-5.6
		All Smokers		
mean	0.56 ± 0.090	0.16 ± 0.033	0.29 ± 0.085	0.19 ± 0.056
range	0.051-8.90	0-3.2	0.017-8.5	0.009-5.6

[a] Values are expressed as mean ± S.E.

Table 5. Urinary NNAL, NNAL glucuronides, and menthol glucuronides in menthol and non-menthol smokers.[a]

Urinary Metabolites[b]	Non-menthol Smokers	Menthol Smokers
NNAL-*N*-Gluc	0.25 ± 0.020	0.33 ± 0.17
(*R*)-NNAL-*O*-Gluc	0.16 ± 0.015	0.17 ± 0.064
(*S*)-NNAL-*O*-Gluc	0.55 ± 0.043	0.57 ± 0.18
Free NNAL	0.15 ± 0.017	0.22 ± 0.11
Total NNAL	1.1 ± 0.083	1.3 ± 0.52
L-MG	11.7 ± 5.5	15.8 ± 2.8
D-MG	0.15 ± 0.065	0.062 ± 0.043
Total-MG	11.9 ± 5.50	15.9 ± 2.8

[a] Values are expressed as mean ± S.E.
[b] Metabolite values are in units of μg/mg creatinine.

DMD Fast Forward. Published on October 2, 2019 as DOI: 10.1124/dmd.119.088351
This article has not been copyedited and formatted. The final version may differ from this version.

Figure Legends

Figure 1. Separation and detection of L- and D-MG. Representative LC-MS/MS chromatograms are shown for a representative *in vitro* DL-menthol (1 mM) incubation with human liver microsomes (panel **A**), and a representative urine specimen from a menthol cigarette smoker (panel **B**). Bottom panels show the LC-MS/MS of the L-menthol glucuronide-d_4 internal standard. Internal standard was spiked into the (HLM) assay prior to quenching the reaction, and was spiked directly into 10 µL of the urine specimen prior to loading onto the LC-MS/MS system.

Figure 2. Levels of menthol glucuronides stratified by menthol and non-menthol cigarette smokers. Levels of L- and D-menthol glucuronides were quantified in the urine of smokers from menthol (n=50) and non-menthol (n=50) cigarette smokers. Menthol glucuronides were analyzed by liquid chromatography-mass spectrometry and were normalized to levels of creatinine. Subjects were stratified by menthol vs. non-menthol smoker groups based on cigarette brand labelling. Panel **A**, menthol and non-menthol branded smoking groups were analyzed for levels of urinary L- and D-menthol glucuronide and normalized based on levels of urinary creatinine. Bars represent mean (± SEM). Panel **B**, histogram showing the number of menthol vs. non-menthol smoking subjects (based on cigarette branding) at different total urinary menthol glucuronide levels. Subjects (non-menthol, n=3) with menthol glucuronide concentrations below the limit of quantification are included in the 0-5 ug/mg creatinine bar. Bars represent the number of subjects in each category. MG, menthol glucuronide.

DMD Fast Forward. Published on October 2, 2019 as DOI: 10.1124/dmd.119.088351
This article has not been copyedited and formatted. The final version may differ from this version.

Figure 3. Levels of NNAL glucuronides stratified by levels of urinary menthol glucuronides. Shown are the urinary levels of NNAL-*N*-Gluc:free NNAL, (*R*)-NNAL-*O*-Gluc:free NNAL, and (*S*)-NNAL-*O*-Gluc:free NNAL in subjects placed into tertiles of low (n=33), intermediate (n=33), and high (n=34) levels of total urinary MG. Total menthol glucuronides (MG), NNAL-*N*-gluc, (*R*)-NNAL-*O*-Gluc, (*S*)-NNAL-*O*-Gluc and free NNAL were analyzed by liquid chromatography-mass spectrometry as described in the Methods. Comparisons of NNAL glucuronide levels were performed using non-parametric ANOVA (NNAL-*N*-Gluc, p=0.011) and a Dunn's posttest (intermediate vs. low and high vs. low). Bars represent mean values (± S.E.). * $p < 0.05$, ** $p < 0.01$.

Figure 4. Inhibition of NNAL-Gluc formation by L- and D-menthol in human liver microsomes. Inhibition of NNAL glucuronides by L- and D-menthol were measured by incubation of NNAL (1mM) in human liver microsomes (HLM) in the presence of varying concentrations of each menthol enantiomer (1.0 µM – 2.5 mM). Representative IC_{50} curves are shown for the inhibition of each NNAL glucuronide formation by L-menthol (x) and D-menthol (•).

DMD Fast Forward. Published on October 2, 2019 as DOI: 10.1124/dmd.119.088351
This article has not been copyedited and formatted. The final version may differ from this version.

Figure 1

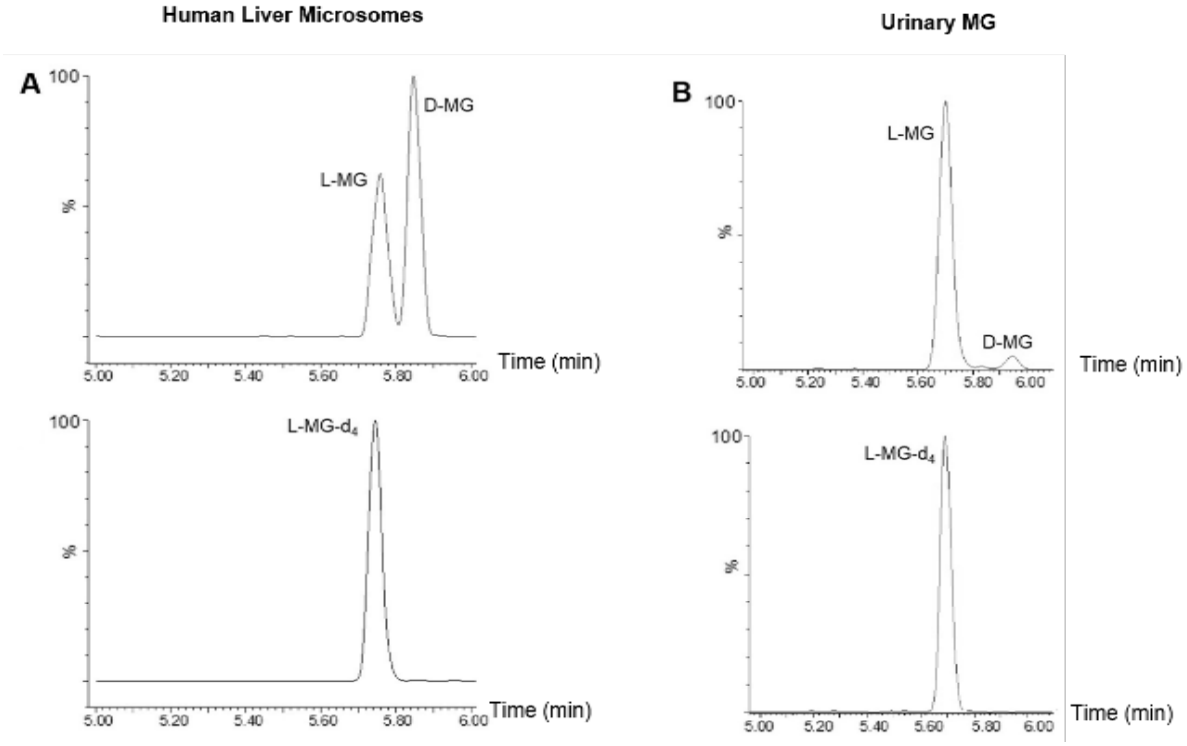

DMD Fast Forward. Published on October 2, 2019 as DOI: 10.1124/dmd.119.088351
This article has not been copyedited and formatted. The final version may differ from this version.

Figure 2

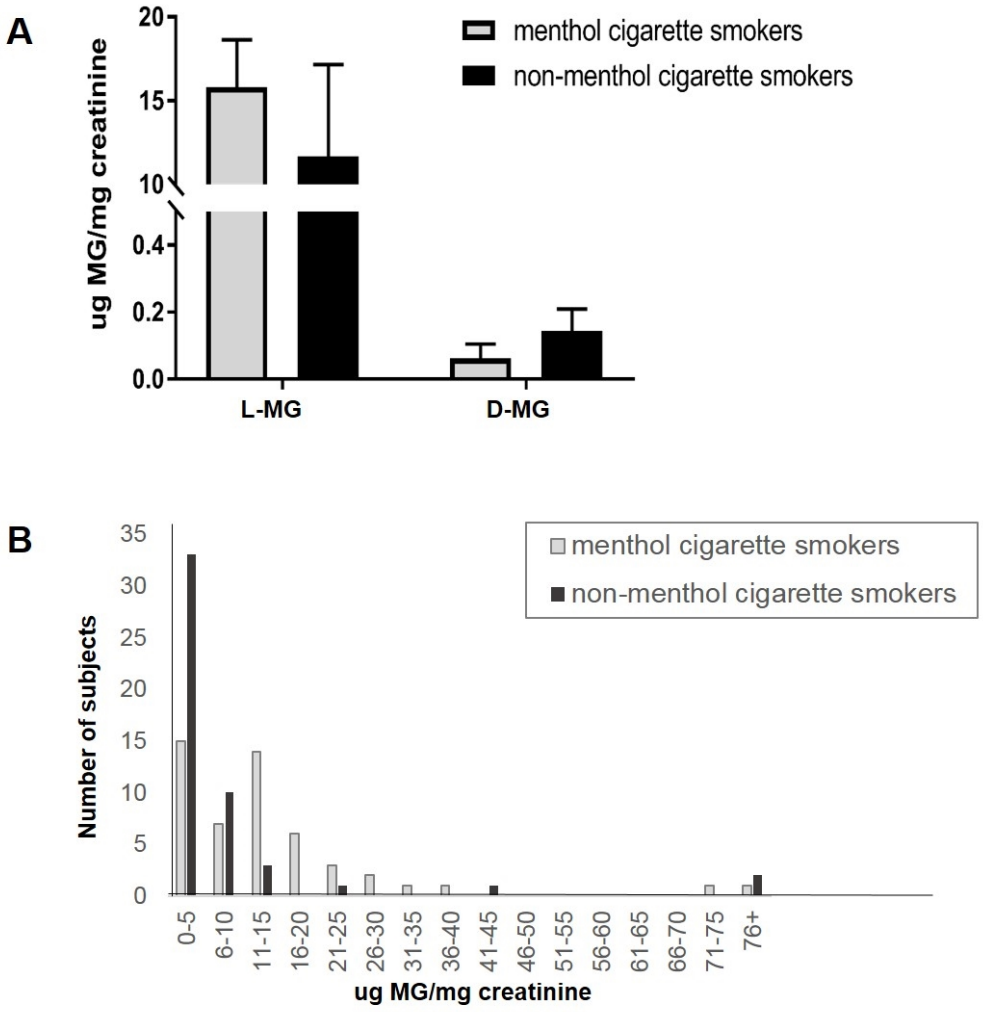

DMD Fast Forward. Published on October 2, 2019 as DOI: 10.1124/dmd.119.088351
This article has not been copyedited and formatted. The final version may differ from this version.

Figure 3

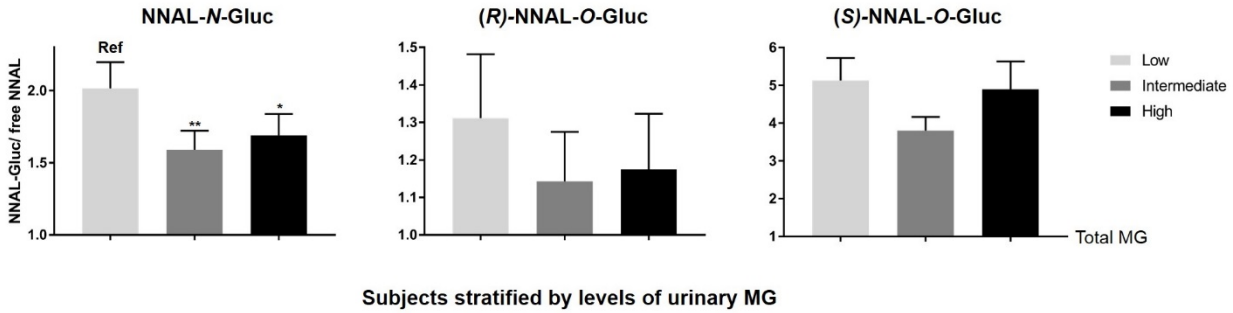

DMD Fast Forward. Published on October 2, 2019 as DOI: 10.1124/dmd.119.088351
This article has not been copyedited and formatted. The final version may differ from this version.

Figure 4